Pergamon

Int. J. Heat Mass Transfer. Vol. 38, No. 11, pp. 2011–2018, 1995

0017-9310/95 $9.50+0.00

0017-9310(94)00313-0

Coriolis effect on free convection in a long rotating porous box subject to uniform heat generation

PETER VADASZ

Department of Mechanical Engineering, University of Durban-Westville, Private Bag X54001, Durban 4000, South Africa

(*Received* 9 *May* 1994 *and in final form* 23 *September* 1994)

Abstract—The Coriolis effect on free convection in a long rotating porous box subject to uniform heat generation is investigated analytically. A three dimensional analytical solution is presented for large values of the porous media Ekman number. The convection results from internal heat generation which produces temperature gradients orthogonal to the centrifugal body force. Two types of thermal boundary conditions are considered for the top and bottom walls of the box. The first type is associated with perfectly conducting boundaries, i.e. the same temperature is imposed on both the top and bottom walls while the second type corresponds to a perfectly conducting top wall and adiabatic bottom wall. The solution to the nonlinear set of partial differential equations is obtained through an asymptotic expansion of the dependent variables in terms of two small parameters representing the reciprocal Ekman number in porous media and the aspect ratio of the domain. Secondary circulation in the form of one or two vortices is obtained in a plane orthogonal to the leading free convection plane.

1. INTRODUCTION

Transport phenomena in rotating porous media have a wide spectrum of applications in engineering and geophysics [1, 2]. The effect of rotation on free convection is of particular interest from both the practical and theoretical points of view.

Research results [3–7] are available for natural convection in rotating porous media resulting from gravity in the presence of a single fluid or binary mixture. However, when a rotating porous matrix is considered, an additional body force exists in the form of the centrifugal acceleration. This force may generate free convection in the same manner as the gravity force causes natural convection. Vadasz [1] presented an analytical solution to the three-dimensional free convection problem in a long rotating porous box by using an asymptotic expansion method. The free convection resulted there from differential heating of the horizontal walls leading to temperature gradients orthogonal to the centrifugal body force. Secondary circulation was obtained in a plane orthogonal to the leading free convection plane as a result of the Coriolis effect on the flow.

This paper presents an analytical investigation of the Coriolis effect on free convection in a long rotating porous box subject to uniform heat generation. The volumetrically uniform heat generation introduces temperature gradients orthogonal to the centrifugal body force while two sets of thermal boundary conditions are considered for the top and bottom walls of the box. The first set considers both walls to be perfectly conducting, i.e. the same value of temperature is imposed on them. The second set considers the top wall to be perfectly conducting and the bottom wall perfectly insulated.

2. PROBLEM FORMULATION

A long rotating fluid saturated porous box subject to uniform heat generation is considered (Fig. 1). At each point of the flow domain the temperatures of the solid and fluid phases are assumed to be equal (Dagan [8]). The front, back and the lateral walls are all insulated. The box has a square cross section of which height and width is H_*, while the subscript * stands for dimensional values. The aspect ratio is defined as $a = H_*/L_*$ where L_* is the length of the box.

Given $\dot{Q}_*$ as the internal rate of heat generation and T_0 as a reference temperature value (e.g. the temperature imposed on the horizontal boundary) the dimensionless temperature can be represented by $T = (T_* - T_0)/(\dot{Q}_* H_*^2/\lambda_{e*})$ where λ_{e*} is the effective thermal conductivity of the porous domain and is assumed constant. Free convection occurs as a result of the centrifugal body force while the gravity force is neglected. The only inertial effects considered are the centrifugal acceleration, as far as changes in density are concerned, and the Coriolis force. Other than that the Darcy's law is assumed to govern the fluid flow (extended to include the centrifugal and Coriolis accelerations), while the Boussinesq approximation is applied for the effects of density variations. As the width (or height) of the domain is much smaller than its length (a small aspect ratio), a Cartesian coordinate

NOMENCLATURE

a	the aspect ratio of the box, equals H_*/L_*
Ek	Ekman number, equals $v_0\phi/2\omega_c k_*$
$\hat{\mathbf{e}}_x$	unit vector in the x direction
$\hat{\mathbf{e}}_y$	unit vector in the y direction
$\hat{\mathbf{e}}_z$	unit vector in the z direction
$\hat{\mathbf{e}}_n$	unit vector normal to the boundary, positive outwards
H_*	the height (width) of the box
k_*	permeability of the porous domain
L_*	the length of the porous domain
M_f	a ratio between the heat capacity of the fluid and the effective heat capacity of the porous domain
p	reduced pressure generalized to include the constant component of the centrifugal term (dimensionless)
$\mathbf{q}$	dimensionless specific flowrate vector equals $u\hat{\mathbf{e}}_x+v\hat{\mathbf{e}}_y+w\hat{\mathbf{e}}_z$
$\dot{Q}_*$	internal rate of heat generation
Ra_ω	porous media Rayleigh number related to the centrifugal body force, equals $\beta_*\dot{Q}_*H_*^3\omega_c^2L_*k_*M_f/\lambda_{e*}\alpha_{e*}\nu_*$
T	dimensionless temperature, equals $(T_*-T_0)\lambda_{e*}/\dot{Q}_*H_*^2$
T_0	a reference temperature value.
u	horizontal x component of the specific flowrate
v	horizontal y component of the specific flowrate
w	vertical component of the specific flowrate
x	horizontal length coordinate
y	horizontal width coordinate
z	vertical coordinate.

Greek symbols

ϕ	porosity
α_{e*}	effective thermal diffusivity
β_*	thermal expansion coefficient
ω_c	angular velocity of the rotating box
ν_*	fluid's kinematic viscosity
μ_*	fluid's dynamic viscosity
ψ	stream function
σ	a dimensionless group, equals Ra_ω/Ek.

Subscripts

*	dimensional values
0	zeroth order
1	first order.

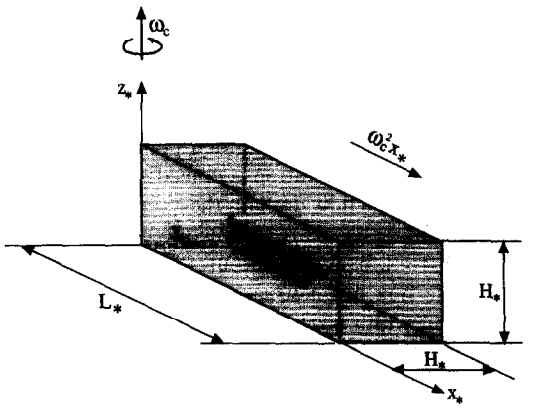

Fig. 1. A long rotating fluid saturated porous box subject to uniform heat generation.

system can be used and the component of the centrifugal acceleration in the y direction can be neglected. The ratio between the centrifugal force component in the y-direction and the corresponding component in the x-direction is $\omega_c^2y_*/\omega_c^2x_* = yH_*/xL_* = (y/x)a$. Therefore for length scales in the x-direction higher than the width of the box $(y/x)a \ll 1$, justifying to neglect the y-component of the centrifugal force. By assuming steady state conditions the following dimensionless set of governing equations is obtained

$$a\frac{\partial u}{\partial x}+\frac{\partial v}{\partial y}+\frac{\partial w}{\partial z}=0 \tag{1}$$

$$u=-\frac{\partial p}{\partial x}-Ra_\omega xT+Ek^{-1}v \tag{2}$$

$$av=-\frac{\partial p}{\partial y}-aEk^{-1}u \tag{3}$$

$$aw=-\frac{\partial p}{\partial z} \tag{4}$$

$$a^2\frac{\partial^2T}{\partial x^2}+\frac{\partial^2T}{\partial y^2}+\frac{\partial^2T}{\partial z^2}-au\frac{\partial T}{\partial x}-v\frac{\partial T}{\partial y}-w\frac{\partial T}{\partial z}+1=0. \tag{5}$$

Equations (1)–(5) are presented in a dimensionless form. The values α_{e*}/H_*M_f, $\mu_*\alpha_{e*}/k_*M_fa$, $\dot{Q}_*H_*^2/\lambda_{e*}$ and $\dot{Q}_*$ are used to scale the specific flowrate components (u_*, v_*, w_*), pressure (p_*), temperature variations (T_*-T_0) and the rate of heat generation, respectively, where α_{e*} is the effective thermal diffusivity, μ_* is the dynamic viscosity, k_* is the permeability of the porous matrix and M_f is the ratio between the heat capacity of the fluid and the effective heat capacity of the porous domain. Two different length scales were applied for scaling the variables x_*, y_* and z_*. Accordingly, $x=x_*/L_*$, $y=y_*/H_*$ and $z=z_*/H_*$. In equations (2) and (3) Ra_ω is the Rayleigh number modified to include the centrifugal body force instead of gravity in the form $Ra_\omega=\beta_*\dot{Q}_*H_*^3\omega_c^2L_*k_*M_f/\lambda_{e*}\alpha_{e*}\nu_*$ and Ek stands for the porous media Ekman number defined by $Ek=\nu_*\phi/2\omega_ck_*$ where ϕ is porosity, ω_c is the angu-

lar velocity of the rotating box, ν_* is the kinematic viscosity of the fluid and β_* is the thermal expansion coefficient.

Two sets of top and bottom boundary conditions are considered while all the sidewalls are kept perfectly insulated.

(*a*) *Boundary conditions—set* 1 (B.C. set 1): *perfectly conducting top and bottom wall*

$$z = 0: \quad T = 0 \quad \text{and} \quad z = 1: \quad T = 0. \tag{6}$$

(*b*) *Boundary conditions—set* 2 (B.C. set 2): *perfectly conducting top wall and adiabatic bottom wall*

$$z = 0: \quad \frac{\partial T}{\partial z} = 0 \quad \text{and} \quad z = 1: \quad T = 0. \tag{7}$$

A third set of boundary conditions representing $z = 0$: $T = 0$ and $z = 1$: $\partial T/\partial z = 0$ is implicitly included in *B.C. set* 2, equation (7) by using the transformation of coordinates $z' = 1 - z$ leading to a solution which is the mirror image (just up side down) of the solution for *B.C. set* 2. It should be mentioned that in most of the practical applications of flows in rotating porous media the Ekman number is usually much greater than 1 and in some applications it is $O(1)$. The significance of the centrifugal force when compared with the gravity is given by the ratio $\omega_c^2 L_*/g_*$. Moreover, the present problem leads to a basic unconditional convection driven by the centrifugal force which is perpendicular to the temperature gradient. The gravity is parallel to the temperature gradient and therefore gravity driven convection becomes possible only for negative temperature gradients (heating from below) and beyond a critical value of the gravity related Rayleigh number.

The partial differential equations (1)–(5) form a nonlinear coupled system. Their coupling is a result of two mechanisms, namely: the Coriolis acceleration and the free convection. While the Coriolis effect causes a linear form of coupling between the horizontal components of the specific flowrates, the free convection coupling between equation (2) and the energy equation (5) introduces the non-linearity.

3. METHOD OF SOLUTION

To obtain an analytical solution to this problem the dependent variables, $\mathbf{q} = u\hat{\mathbf{e}}_x + v\hat{\mathbf{e}}_y + w\hat{\mathbf{e}}_z$ ($\hat{\mathbf{e}}_x$, $\hat{\mathbf{e}}_y$ and $\hat{\mathbf{e}}_z$ are unit vectors in the x, y and z directions, respectively), T and p are expanded in a double power series in terms of two small parameters representing the reciprocal Ekman number in porous media and the aspect ratio of the domain ($Ek \gg 1$, $a \ll 1$), in the form

$$[\mathbf{q}, T, p] = \sum_{m=0}^{\infty} \sum_{n=0}^{\infty} a^m Ek^{-n} [\mathbf{q}_{mn}, T_{mn}, p_{mn}]. \tag{8}$$

As all the boundaries are rigid the solution must obey the impermeability conditions there, i.e. $\mathbf{q} \cdot \hat{\mathbf{e}}_n = 0$ on the boundaries, where $\hat{\mathbf{e}}_n$ is a unit vector normal to the boundary. The thermal boundary conditions at the sidewalls are: $\nabla T \cdot \hat{\mathbf{e}}_n = 0$, representing the insulation condition on these walls, while the thermal boundary conditions at the top and bottom boundaries are as specified in equation (6) for *B.C. set* 1 or equation (7) for *B.C. set* 2. By introducing the expansion (8) into equations (1)–(5) a hierarchy of partial differential equations is obtained for the different orders.

3.1. *The leading order*

To leading order the zero powers of a^m and Ek^{-n} are used, which yields a reduced set of equations. At this order $v_{oo} = w_{oo} = 0$ and the energy equation (5) becomes

$$\frac{d^2 T_{oo}}{dz^2} + 1 = 0 \tag{9}$$

leading to the following solutions for T_{oo} corresponding to the two sets of boundary conditions

(*a*) *for boundary conditions—set* 1

$$T_{oo} = \tfrac{1}{2} z(1 - z); \tag{10}$$

(*b*) *for boundary conditions—set* 2

$$T_{oo} = \tfrac{1}{2}(1 - z^2). \tag{11}$$

Accordingly equations (2)–(4) give

$$\frac{\partial u_{oo}}{\partial z} = -Ra_\omega x \frac{\partial T_{oo}}{\partial z}. \tag{12}$$

By assuming that u_{oo} has the form $u_{oo} = x\zeta_{oo}(z)$, substituting it and T_{oo} from equations (10) and (11) into equation (12) and integrating yields

(*a*) *for boundary conditions—set* 1

$$\zeta_{oo} = \frac{Ra_\omega}{2} z(z - 1) + C_1; \tag{13}$$

(*b*) *for boundary conditions—set* 2

$$\zeta_{oo} = \frac{Ra_\omega}{2} z^2 + C_2 \tag{14}$$

where C_1 and C_2 are constants of integration which are evaluated by using the integral condition stating that the net flowrate over any cross section is zero, i.e.

$$\int_0^1 \zeta_{oo}\, dz = 0 \tag{15}$$

leading to the following solutions for u_{oo}:

(*a*) *for boundary conditions—set* 1

$$u_{oo} = \frac{Ra_\omega x}{2} [z^2 - z + \tfrac{1}{6}]; \tag{16}$$

(*b*) *for boundary conditions—set* 2

$$u_{oo} = \frac{Ra_\omega x}{2} [z^2 - \tfrac{1}{3}]. \tag{17}$$

The graphical description of the leading order solutions T_{oo} [equations (10) and (11)] and u_{oo}/xRa_ω

[equations (16) and (17)] for the corresponding sets of boundary conditions is presented in Fig. 2. These solutions represent the free convection in the core region, i.e. far from the sidewalls $x_* = 0$ or $x_* = L_*$. The solution next to the sidewalls at $x = 0$ and $x = 1$ can be evaluated using a boundary layer matching method as suggested by Bejan and Tien [9], Cormack *et al.* [10, 11] and Imberger [12]. Such a matching procedure based on the method of integral of momentum was applied by Vadasz [1] to the corresponding problem without heat generation.

3.2. *First order in* Ek^{-n}

As the main objective of this paper is to investigate the Coriolis effect on the free convection, the following analysis focuses on the solution to order 1 in Ek^{-n} and to order 0 in a^m. Therefore, the corresponding equations are presented in the form

$$\frac{\partial v_{01}}{\partial y} + \frac{\partial w_{01}}{\partial z} = 0 \tag{18}$$

$$u_{01} = -\frac{\partial p_{01}}{\partial x} - Ra_\omega x T_{01} + v_{00}; \quad \frac{\partial p_{01}}{\partial y} = 0; \quad \frac{\partial p_{01}}{\partial z} = 0 \tag{19}$$

$$\frac{\partial^2 T_{01}}{\partial y^2} + \frac{\partial^2 T_{01}}{\partial z^2} = w_{01}\frac{\mathrm{d}T_{00}}{\mathrm{d}z}. \tag{20}$$

To obtain a solution for v_{01} and w_{01} one should refer to the equations at orders 1 in a^m and 1 in Ek^{-n} leading to

$$v_{01} = -\frac{\partial p_{11}}{\partial y} - u_{00}; \quad w_{01} = -\frac{\partial p_{11}}{\partial z}. \tag{21}$$

The pressure is eliminated from these equations by taking the derivatives $\partial/\partial z$ and $\partial/\partial y$ of v_{01} and w_{01} in equation (21), respectively and subtracting. By introducing the stream function to satisfy identically equation (18), i.e. $v_{01} = \partial\psi_{01}/\partial z$, $w_{01} = -\partial\psi_{01}/\partial y$, one obtains

$$\frac{\partial^2 \psi_{01}}{\partial y^2} + \frac{\partial^2 \psi_{01}}{\partial z^2} = -\frac{\partial u_{00}}{\partial z}. \tag{22}$$

The sequence of operations applied for the solution at this order is as follows:

(1) substitution of u_{00} from the leading order solutions (16) and (17) into equation (22);
(2) analytical solution of equation (22) for ψ_{01} (subject to the impermeability boundary conditions on the rigid walls, i.e. $\psi_{01} = 0\ \forall\ (y = 0,1; z = 0,1)$) and its corresponding derivatives v_{01} and w_{01};
(3) substitution of w_{01} (evaluated in step (2)) and T_{00} from the leading order solutions (10) and (11) into equation (20);
(4) analytical solution of equation (20) for T_{01};
(5) substitution of T_{01} (evaluated in step (4)) and the leading order solution v_{00} (see text preceding equation (9)) into equations (19); and
(6) analytical solution of equations (19) for u_{01}.

This sequence of operations leads to the following solutions for ψ_{01} and consequently for v_{01} and w_{01}.

(*a*) *For boundary conditions—set* 1

$$\psi_{01} = -\frac{4Ra_\omega x}{\pi^4}\sum_{i=1}^{\infty}\sum_{j=1}^{\infty}\frac{\sin[(2i-1)\pi y]\sin[2j\pi z]}{j(2i-1)[4j^2+(2i-1)^2]} \tag{23}$$

$$v_{01} = \frac{\partial\psi_{01}}{\partial z} = -\frac{8Ra_\omega x}{\pi^3} \times \sum_{i=1}^{\infty}\sum_{j=1}^{\infty}\frac{\sin[(2i-1)\pi y]\cos[2j\pi z]}{(2i-1)[4j^2+(2i-1)^2]} \tag{24}$$

$$w_{01} = -\frac{\partial\psi_{01}}{\partial y} = \frac{4Ra_\omega x}{\pi^3} \times \sum_{i=1}^{\infty}\sum_{j=1}^{\infty}\frac{\cos[(2i-1)\pi y]\sin[2j\pi z]}{j[4j^2+(2i-1)^2]}. \tag{25}$$

(*b*) *For boundary conditions—set* 2

$$\psi_{01} = \frac{8Ra_\omega x}{\pi^4}\sum_{i=1}^{\infty}\sum_{j=1}^{\infty}\frac{(-1)^{j+1}\sin[(2i-1)\pi y]\sin[j\pi z]}{j(2i-1)[j^2+(2i-1)^2]} \tag{26}$$

$$v_{01} = \frac{\partial\psi_{01}}{\partial z} = \frac{8Ra_\omega x}{\pi^3} \times \sum_{i=1}^{\infty}\sum_{j=1}^{\infty}\frac{(-1)^{j+1}\sin[(2i-1)\pi y]\cos[j\pi z]}{(2i-1)[j^2+(2i-1)^2]} \tag{27}$$

$$w_{01} = -\frac{\partial\psi_{01}}{\partial y} = -\frac{8Ra_\omega x}{\pi^3} \times \sum_{i=1}^{\infty}\sum_{j=1}^{\infty}\frac{(-1)^{j+1}\cos[(2i-1)\pi y]\sin[j\pi z]}{j[j^2+(2i-1)^2]}. \tag{28}$$

Substitution of w_{01} from equations (25) and (28) into equation (20), and of T_{00} from equations (10) and (11) into equation (20) yields a Poisson type of equation for T_{01}. Its solution was obtained analytically by using the method of separation of variables and is presented in the form

(*a*) *for boundary conditions—set* 1

$$T_{01} = Ra_\omega x\sum_{i=1}^{\infty}\sum_{k=1}^{\infty}b_{ik}\cos[(2i-1)\pi y]\sin[k\pi z] \tag{29}$$

where

$$b_{ik} = -\frac{32k}{\pi^5[(2i-1)^2+k^2]} \times \sum_{\substack{j=1\\ j\neq k/2}}^{\infty}\frac{[2(-1)^{k+1}+[(4j^2-k^2)^2\pi^2]^{-1}]}{[4j^2+(2i-1)^2]}; \tag{30}$$

(*b*) *for boundary conditions—set* 2

$$T_{01} = Ra_\omega x\sum_{i=1}^{\infty}\sum_{k=1}^{\infty}b_{ik}\cos[(2i-1)\pi y]\cos\left[\frac{k\pi z}{2}\right] \tag{31}$$

where

$$b_{ik} = \frac{64}{\pi^7\left[(2i-1)^2+\frac{k^2}{4}\right]} \times \sum_{j=1}^{\infty} \frac{(-1)^{j+k+1}(4j^2+k^2)}{j[j^2+(2i-1)^2](2j-k)^2(2j+k)^2}. \quad (32)$$

To evaluate u_{01} the leading order solution $v_{00} = 0$ and T_{01} given by equations (29) and (31) are substituted into equations (19) leading to

$$u_{01} = -\frac{dp_{01}}{dx} - Ra_\omega x T_{01}. \quad (33)$$

Following equation (19) the pressure gradient dp_{01}/dx is represented as an ordinary derivative. Any solution for u_{01} must satisfy an integral condition of mass conservation stating that the net flowrate over any cross section is zero, i.e.

$$\int_0^1 \int_0^1 u_{01}\, dy\, dz = 0. \quad (34)$$

Substituting equation (33) for u_{01} into the integral in equation (34) yields

$$\int_0^1 \int_0^1 \frac{dp_{01}}{dx} dy\, dz + Ra_\omega x \int_0^1 \int_0^1 T_{01}\, dy\, dz = 0. \quad (35)$$

The first integral in equation (35) equals dp_{01}/dx, while the second integral vanishes for both *set* 1 and *set* 2 of boundary conditions. As a result it can be established from equation (35) that $dp_{01}/dx = 0$. Substituting this result into equation (33) gives the solution of u_{01} in the form

$$u_{01} = -Ra_\omega x T_{01} \quad (36)$$

where T_{01} is given by equation (29) for *B.C. set* 1 and by equation (31) for *B.C. set* 2.

3.3. *Combined solution*

Finally the complete solution up to and including order 1 in Ek^{-n} is obtained by substitution of the leading order and first order solutions into equation (8) and is presented in the form

(a) for boundary conditions—set 1

$$\frac{u}{Ra_\omega x} = -\tfrac{1}{2}[z^2 - z + \tfrac{1}{6}] - \frac{Ra_\omega x}{Ek}\sum_{i=1}^{\infty}\sum_{k=1}^{\infty} b_{ik}\cos[(2i-1)\pi y]\sin[k\pi z] \quad (37)$$

$$v = -\frac{8Ra_\omega x}{\pi^3 Ek}\sum_{i=1}^{\infty}\sum_{j=1}^{\infty}\frac{\sin[(2i-1)\pi y]\cos[2j\pi z]}{(2i-1)[4j^2+(2i-1)^2]} \quad (38)$$

$$w = \frac{4Ra_\omega x}{\pi^3 Ek}\sum_{i=1}^{\infty}\sum_{j=1}^{\infty}\frac{\cos[(2i-1)\pi y]\sin[2j\pi z]}{j[4j^2+(2i-1)^2]} \quad (39)$$

$$T = \tfrac{1}{2}z[1-z] + \frac{Ra_\omega x}{Ek}\sum_{i=1}^{\infty}\sum_{k=1}^{\infty} b_{ik}\cos[(2i-1)\pi y]\sin[k\pi z] \quad (40)$$

where b_{ik} for this set of boundary conditions is the coefficient given by equation (30).

(b) For boundary conditions—set 2

$$\frac{u}{Ra_\omega x} = \tfrac{1}{2}[z^2 - \tfrac{1}{3}] - \frac{Ra_\omega x}{Ek}\sum_{i=1}^{\infty}\sum_{k=1}^{\infty} b_{ik}\cos[(2i-1)\pi y]\cos\left[\frac{k\pi z}{2}\right] \quad (41)$$

$$v = \frac{8Ra_\omega x}{\pi^3 Ek}\sum_{i=1}^{\infty}\sum_{j=1}^{\infty}\frac{(-1)^{j+1}\sin[(2i-1)\pi y]\cos[j\pi z]}{(2i-1)[j^2+(2i-1)^2]} \quad (42)$$

$$w = -\frac{8Ra_\omega x}{\pi^3 Ek}\sum_{i=1}^{\infty}\sum_{j=1}^{\infty}\frac{(-1)^{j+1}\cos[(2i-1)\pi y]\sin[j\pi z]}{j[j^2+(2i-1)^2]} \quad (43)$$

$$T = \tfrac{1}{2}[1-z^2] + \frac{Ra_\omega x}{Ek}\sum_{i=1}^{\infty}\sum_{k=1}^{\infty} b_{ik}\cos[(2i-1)\pi y]\cos\left[\frac{k\pi z}{2}\right] \quad (44)$$

where b_{ik} for this set of boundary conditions is the coefficient given by equation (32).

From these solutions one observes that the Coriolis effect appears as a correction of the free convection solutions as far as u and T are concerned. However it generates a flow in the yz plane which is perpendicular to the original free convection flow. Under the asymptotic conditions prevailing in this investigation the flow in the yz plane can be represented by a stream function $\psi = Ek^{-1}\psi_{01}$, where ψ_{01} is the solution given by equations (23) and (26) for the first and second set of boundary conditions, respectively. Another observation which can be made from the combined solutions represented by equations (37)–(44) is that in the context of the asymptotic conditions the Coriolis effect on free convection is controlled by the combined dimensionless group $\sigma = Ra_\omega Ek^{-1}$, i.e.

$$\sigma = \frac{Ra_\omega}{Ek} = \frac{2\beta_* \dot{Q}_* H^3 \omega_c^3 L_* k_*^2 M_f}{\lambda_{e*}\alpha_{e*}\nu_*^2\phi}. \quad (45)$$

The validity of the asymptotic expansion is restricted too, by the values of σ and the expansion is valid for $Ek \gg 1$ as long as the value of a is small as well.

4. RESULTS AND DISCUSSION

The analytical solutions obtained in the previous section are presented graphically in Figs. 2–6 and their significance is discussed in this section.

The leading order core solutions $u_{00}/Ra_\omega x$ and T_{00} are presented in Fig. 2. The horizontal flow in the x direction, Fig. 2(a) and (c), represents the free convection resulting from the temperature gradient,

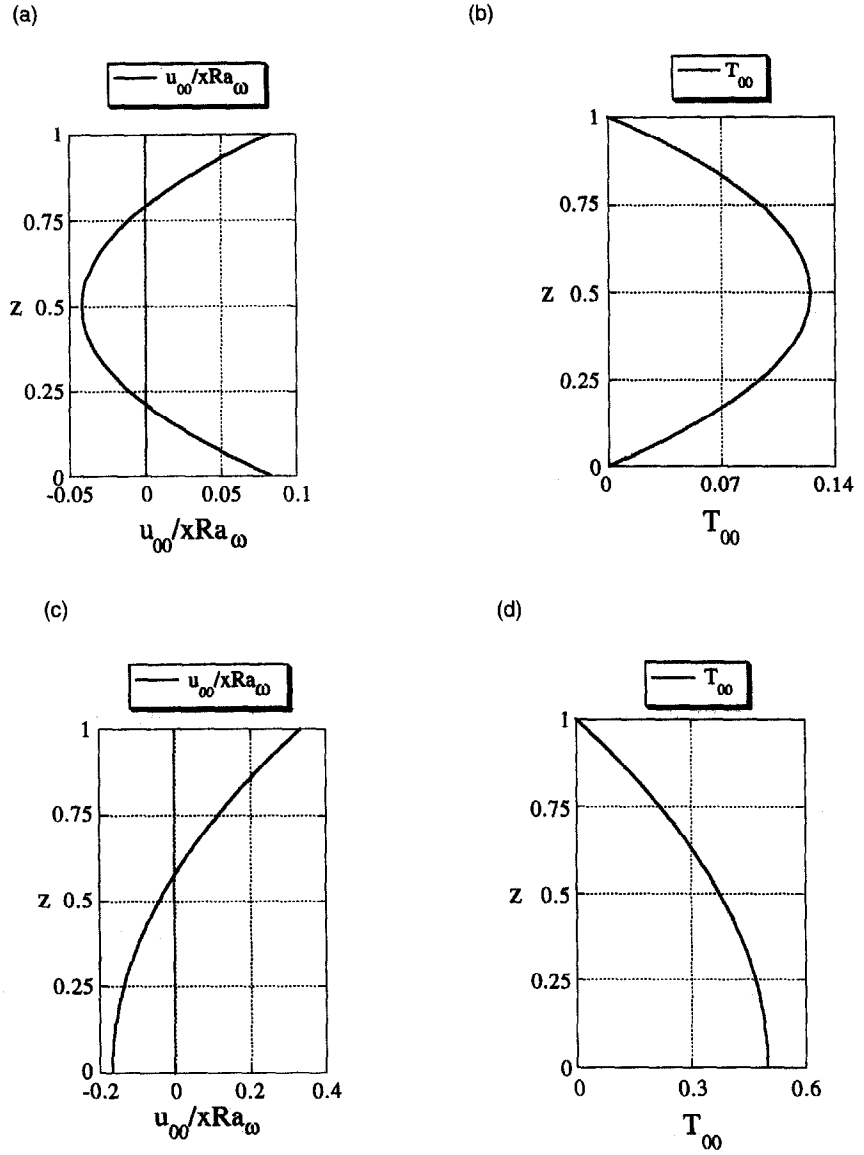

Fig. 2. Graphical description of the free convection flow and temperature fields at the leading order; (a) the horizontal x component of the specific flowrate u_{00} for *B.C. set* 1; (b) the temperature profile T_{00} for *B.C. set* 1; (c) the horizontal x component of the specific flowrate u_{00} for *B.C. set* 2; (d) the temperature profile T_{00} for *B.C. set* 2.

Fig. 2(b) and (d), created by the uniform heat generation. Figure 2(a) and (b) corresponds to *B.C. set* 1 while Fig. 2(c) and (d) corresponds to *B.C. set* 2. According to the results corresponding to *B.C. set* 1 a core flow moving in a direction opposite to the centrifugal acceleration is generated by the high temperatures in this core region ($z \in [0.211, 0.789]$) while a flow in the same direction as the centrifugal acceleration is obtained next to the boundaries ($z \in [0., 0.211]$ and $z \in [0.789, 1.]$). Regarding the results corresponding to *B.C. set* 2, a flow opposite to the direction of the centrifugal acceleration is obtained in the bottom hot part of the domain ($z \in [0., 0.577]$), while the flow changes direction in the colder upper part of the domain ($z \in [0.577, 1.]$). The Coriolis effect is felt at order 1 in Ek^{-n} leading to secondary circulation in a plane orthogonal to the leading free convection plane. As a result, the leading order convection occurring in the xz plane induces through the Coriolis effect a secondary motion in the yz plane. The graphical description of this secondary flow field at any cross section, represented by constant values of $\psi\pi^4/4\sigma x$ and corresponding to *B.C. set* 1, is presented in Fig. 3. Two vortices are a result of the sign variation of the temperature gradient at the leading order, the bottom vortex rotating clockwise while the top vortex rotates anti-clockwise. A steeper vertical gradient of the stream function, representing a stronger horizontal

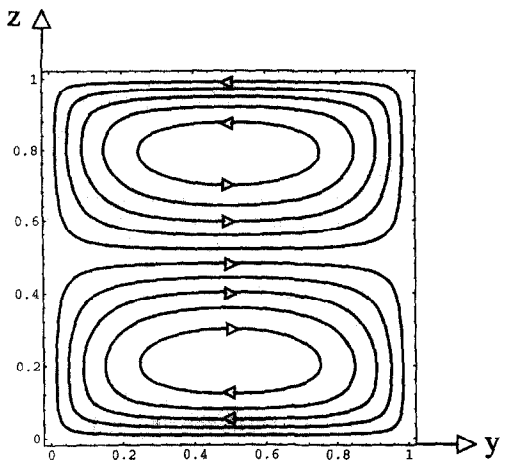

Fig. 3. Graphical description of the flow field at any cross section represented by constant values of $\psi\pi^4/4\sigma x$ and corresponding to *B.C. set* 1. Ten streamlines equally divided between their minimum value of $(\psi\pi^4/4\sigma x)_{\min} = -0.188$ and their maximum value of $(\psi\pi^4/4\sigma x)_{\max} = 0.188$.

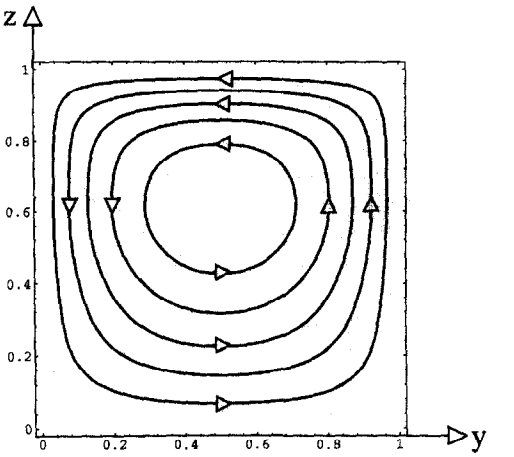

Fig. 5. Graphical description of the flow field at any cross section represented by constant values of $\psi\pi^4/8\sigma x$ and corresponding to *B.C. set* 2. Five streamlines equally divided between their minimum value of $(\psi\pi^4/8\sigma x)_{\min} = 0$ and their maximum value of $(\psi\pi^4/8\sigma x)_{\max} = 0.489$.

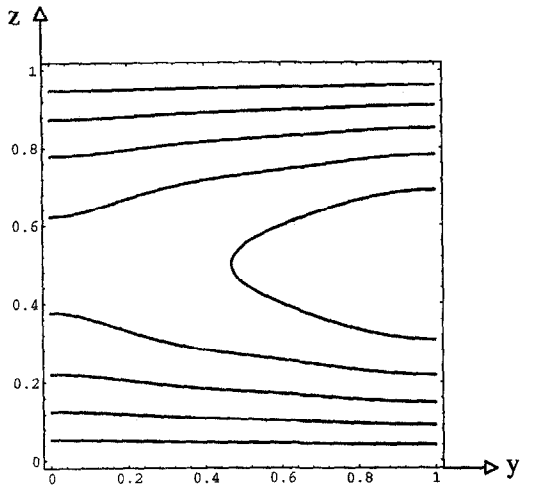

Fig. 4. Graphical description of the temperature field T on the yz plane corresponding to *B.C. set* 1 and to $\sigma x = 0.5$. Five isotherms equally divided between $T_{\min} = 0$ and $T_{\max} = 0.149$.

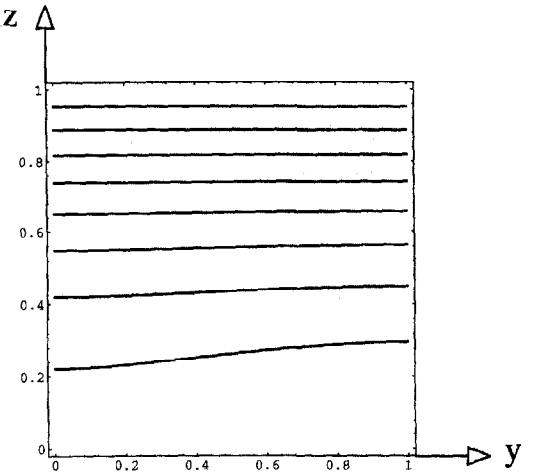

Fig. 6. Graphical description of the temperature field T on the yz plane corresponding to *B.C. set* 2 and to $\sigma x = 2$. Eight isotherms equally divided between $T_{\min} = 0$ and $T_{\max} = 0.525$.

flow, is observed next to the walls at $z = 0$ and $z = 1$, while the gradient becomes moderate as one moves away from these boundaries. The reason behind this result, which is asymmetric with respect to the center of the vortex, lies in the forcing term of equation (22). There, it is clear that the stream function in the yz plane, ψ_{01}, is affected by the gradient of the flow at the leading order, i.e. $(-\partial u_{00}/\partial z)$. Since this gradient is steep at $z = 0$ and $z = 1$, see Fig. 2(a), the same applies for the stream function as well. As a result of this circulation the temperature distribution is affected significantly. The graphical description of the temperature field, T, on the yz plane corresponding to *B.C. set* 1 and for $\sigma x = 0.5$ is presented in Fig. 4. The effect of convection is apparent in this figure as the distortion of the isotherms from the parallel horizontal form prevailing to a conduction regime is significant. A totally different secondary motion in the yz plane is obtained for *B.C. set* 2. The graphical description of this secondary flow field at any cross section, represented by constant values of $\psi\pi^4/8\sigma x$ and corresponding to *B.C. set* 2 is presented in Fig. 5. A single vortex rotating anti-clockwise represents the solution according to set 2 of boundary conditions, the reason of which is the leading order temperature distribution being monotonic, see Fig. 2(d). In this case a steep vertical gradient of the stream function, representing a stronger horizontal flow, is observed next to the top wall while the gradient becomes moderate as one moves away from this wall. The vertical asymmetry of the flow associated with this result is caused by the forcing term in equation (22). Since according to equation (22) the stream function in the

yz plane is affected by the gradient of the horizontal flow at the leading order, i.e. $(-\partial u_{00}/\partial z)$ and the latter is steep at $z = 1$ and becomes moderate far away from this wall, see Fig. 2(c), the same applies for the stream function as well. The effect of this secondary flow on the temperature field in the yz plane is presented in Fig. 6 where the effect of convection on the isotherms is felt as well. It is worthwhile to mention that the separation between the flow in the yz plane and the convection in the x direction was possible due to the large Ekman number considered. Nevertheless, in general, rotating flows have a tendency towards two dimensionality, as shown by Greenspan [13] for rotating flows in pure fluids (non-porous domains) and by Vadasz [14] for rotating flows in porous media.

5. CONCLUSIONS

A three-dimensional analytical solution demonstrating the Coriolis effect on free convection in a long rotating porous box subject to uniform heat generation was presented for high values of the porous media Ekman number. Free convection is a result of the internal heat generation which produces temperature gradients perpendicular to the centrifugal body force. Secondary circulation was obtained in a plane perpendicular to the leading free convection plane in the form of one or two vortices associated with the type of top and bottom boundary conditions considered.

Acknowledgement—The author wishes to thank the Foundation for Research Development for funding this research through the Core Programme Rolling Grant.

REFERENCES

1. P. Vadasz, Three-dimensional free convection in a long rotating porous box, *J. Heat Transfer* **115**, 639–644 (1993).
2. P. Vadasz, Fluid flow through heterogeneous porous media in a rotating square channel, *Transp. Porous Media* **12**, 43–54 (1993).
3. P. R. Patil and G. Vaidyanathan, On setting up of convection currents in a rotating porous medium under the influence of variable viscosity, *Int. J. Engng Sci.* **21**, 123–130 (1983).
4. J. J. Jou and J. S. Liaw, Transient thermal convection in a rotating porous medium confined between two rigid boundaries, *Int. Commun. Heat Mass Transfer* **14**, 147–153 (1987).
5. J. J. Jou and J. S. Liaw, Thermal convection in a porous medium subject to transient heating and rotation, *Int. J. Heat Mass Transfer* **30**, 208–211 (1987).
6. N. Rudraiah, I. S. Shivakumara and R. Friedrich, The effect of rotation on linear and non-linear double-diffusive convection in sparsely packed porous medium, *Int. J. Heat Mass Transfer* **29** (9), 1301–1317 (1986).
7. E. Palm and A. Tyvand, Thermal convection in a rotating porous layer, *J. Appl. Math. Phys.* (ZAMP) **35**, 122–123 (1984).
8. G. Dagan, Some aspects of heat and mass transfer in porous media. In *Fundamentals of Transport Phenomena in Porous Media*. Elsevier, Amsterdam (1972).
9. A. Bejan and C. L. Tien, Natural convection in a horizontal porous medium subjected to an end-to-end temperature difference, *ASME J. Heat Transfer* **100**, 191–198 (1978).
10. D. E. Cormack, L. G. Leal and J. Imberger, Natural convection in a shallow cavity with differentially heated end walls—I. Asymptotic theory, *J. Fluid Mech.* **65**, 209–229 (1974).
11. D. E. Cormack, L. G. Leal and J. H. Seinfeld, Natural convection in a shallow cavity with differentially heated end walls—II. Numerical solutions, *J. Fluid Mech.* **65**, 231–246 (1974).
12. J. Imberger, Natural convection in a shallow cavity with differentially heated end walls III. Experimental results, *J. Fluid Mech.* **65**, 247–260 (1974).
13. H. P. Greenspan, *The Theory of Rotating Fluids*. Cambridge University Press, Cambridge (1980).
14. P. Vadasz, On Taylor–Proudman columns and geostrophic flow in rotating porous media, *SAIMechE R&D J.* **10**, 53–57 (1994).